

Appendix F – Detailed Reply to Peer Review Comment #75

Reviewer Murley commented that “to better understand the PFM results it would be useful to see examples where the progress of a crack through the vessel wall is tracked.” In this Appendix we discuss four transients for which we track the progress (or lack thereof) of various simulated cracks through the vessel wall. One transient was selected from each of the four dominant transient classes:

- Primary side pipe break
 - Beaver Valley transient 07
 - 8 in. surge line break
- Stuck-open valve on the primary side
 - Oconee transient 122
 - Stuck-open pressurizer safety valve that recloses at 6000 seconds. Operator throttles HPI 10 minutes after reaching the throttling criteria
- Main steam line break
 - Beaver Valley transient 104
 - Main steam line break with AFW continuing to feed affected generator for 30 minutes. Operator controls HHSI 60 minutes after allowed. Break is assumed to occur inside containment so that the operator trips the RCPs due to adverse containment conditions
- Stuck-open valve on the secondary side
 - Palisades transient 55
 - Turbine/reactor trip with 2 stuck-open ADVs on SG-A combined with controller failure resulting in the flow from two AFW pumps into affected steam generator. Operator starts second AFW pump.

We selected flaws to track to illustrate the various features of the FAVOR crack initiation/arrest/reinitiat/rearrest model. In FAVOR flaws can initiate (start moving through the vessel wall), arrest (stop moving through the vessel wall), and ultimately fail the vessel in a number of different ways:

- Cracks can **initiate from original fabrication flaws** only by cleavage fracture (i.e., K_I exceeds K_{Ic}). Note that the criteria for cleavage crack initiation also requires that K_I be rising when it exceeds K_{Ic} . If K_I is falling when it exceeds K_{Ic} a condition exists called “warm pre-stress” and crack initiation can no longer occur. In principal crack initiation by ductile mechanisms is also possible (i.e., K_I exceeds $K_{I(JIc)}$). However for the combinations of flaw sizes, loadings, and toughness conditions considered in this project initiation from an original fabrication flaw by ductile mechanisms has never been simulated.
- Cracks **arrest** whenever the driving force (K_I) falls below the cleavage crack arrest toughness (K_{Ia}).
- Once arrested, cracks can **reinitiate** by one of two mechanisms
 - Cracks can reinitiate in cleavage (see description under *initiate from original fabrication flaws* above).
 - Cracks can reinitiate by ductile tearing if the applied driving force exceeds the ductile crack initiation toughness (i.e., if K_I exceeds $K_{I(JIc)}$).

Note that the mode of crack reinitiat is controlled by the lesser of the cleavage crack initiation toughness and the ductile crack initiation toughness.

- Once reinitiated, cracks can **rearrest** by one of two mechanisms
 - Cracks can rearrest in cleavage (see description under *arrest* above).
 - Cracks can rearrest due to inadequate driving force to continue propagation of a ductile crack.

Note that the mode of crack rearrest is controlled by the mode of crack reinitiat.

- The crack initiation/arrest/reinitiat/rearrest process continues until either a stable arrest is achieved somewhere in the vessel wall or the vessel is simulated to fail. **Through-wall cracking (failure) of the vessel** can occur by any of the following three mechanisms:
 - Net-section collapse of the ligament between the crack tip and the vessel OD can occur (tensile instability).
 - Ductile tearing can become structurally unstable
 - The crack can advance by either cleavage or ductile mechanisms to a user-specified fraction of the total wall thickness. In the analyses reported herein that fraction is set to 90%. Accurate solution of the fracture driving force equations for very deep cracks is not possible, necessitating use of this cut-off value.

Details of all of the fracture models can be found in both [EricksonKirk 10-03] and in [Williams 10-03].

The remaining pages of this appendix track the progress (or lack thereof) of various simulated cracks through the vessel wall for the transients described earlier.

Deterministic analysis of a simulated flaw subjected to Beaver Valley transient 07 at 60 EFY

Transient sequence:	Beaver Valley 07	
Transient Description:	8 in. surge line break (See Figure 7.1 for pressure and temperature variation)	
Flaw Analyzed:	Orientation:	Axial
	Type:	Embedded flaw in plate material
	Depth (2a):	0.321 in
	Length (2c):	0.446 in
	Inner crack tip distance from ID (ℓ):	0.218 in
Embrittlement:	EFY:	60 years
	Simulated RT_{NDT} at inner crack tip	279°F

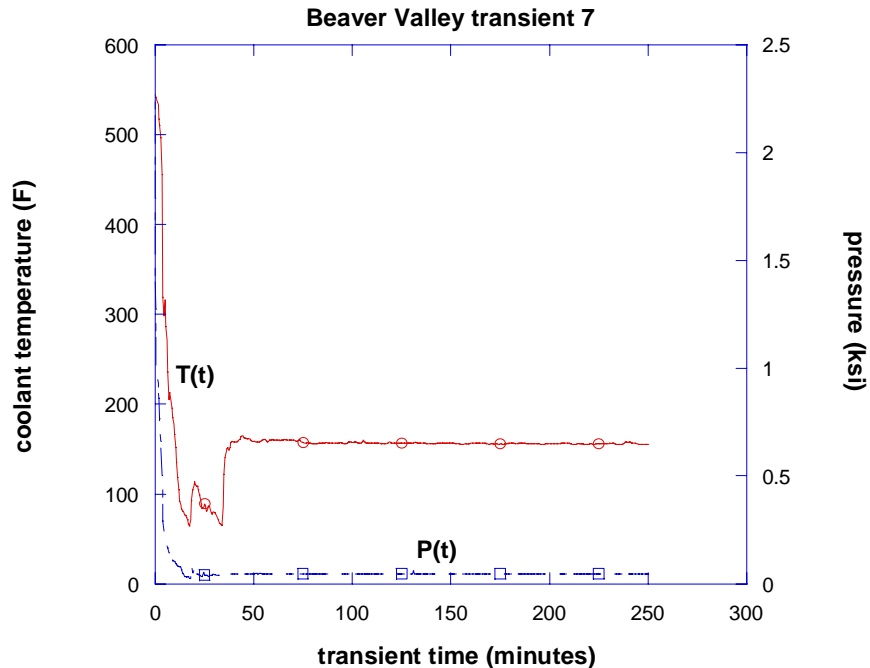


Figure 7.1 – Beaver Valley transient sequence 7 – 8 in. surge line break

Crack Initiation

Figure 7.2 illustrates that the conditions for the flaw to have a conditional probability of crack initiation (cpi) > 0 are satisfied: (1) the applied driving force to fracture (K_I) is greater than the minimum of the cleavage fracture initiation toughness (K_{Ic}) distribution (which corresponds to the Weibull ‘a’ parameter), and (2) during the time that applied K_I is greater than the minimum K_{Ic} , the applied K_I must also be greater than at all previous time steps. The second condition is a necessary condition to overcome effect of warm-prestress.

Figure 7.2 illustrates that the flaw has a conditional probability of initiation (cpi) > 0 in the transient time interval between 10 and 12 minutes. The flaw cannot initiate before a transient time of 10 minutes since this is the first time step at which K_I exceeds the minimum value of K_{Ic} . The flaw cannot initiate after a transient time of 12 minutes because this is the time at which the maximum applied K_I occurs, producing a condition of warm-prestress.

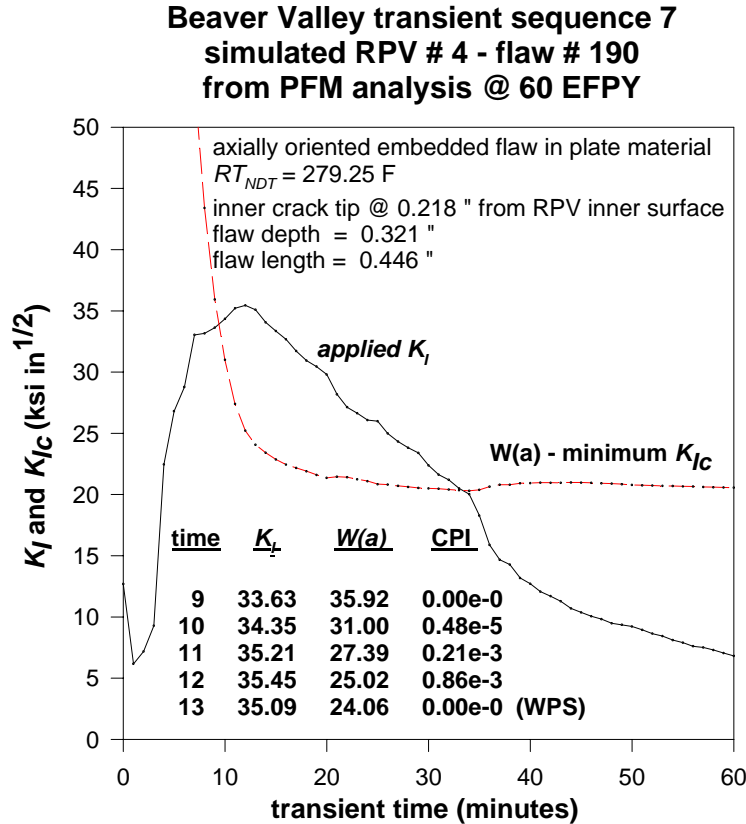


Figure 7.2 – Beaver Valley transient sequence 7 – deterministic LEFM analysis for flaw from PFM Monte Carlo analysis for which $cpi > 0$

Through-Wall Cracking Analysis #1:

This is one simulation of the through-wall cracking behavior of the flaw initiated in Figure 7.2. This analysis occurs at $t=12$ minutes.

Event 1: Figure 7.3(a) illustrates that the initiated flaw propagates through the wall thickness to failure since the applied driving force to fracture (K_I) exceeds the crack arrest toughness (K_{Ia}) through the entire wall thickness at $t=12$ minutes.

**Flaw 190; arrest trial 67; time = 12 minutes
initiated flaw propagates to failure by cleavage fracture
with no arrest
(failure defined as flaw propagating 90% of wall thickness)**

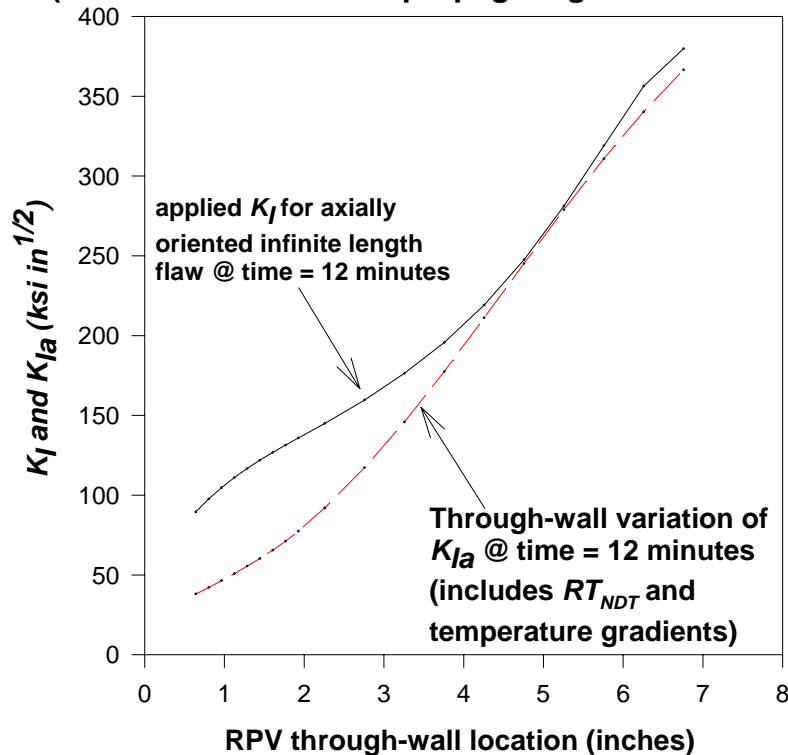


Figure 7.3 – Beaver Valley transient sequence 7 – deterministic through-wall analysis for flaw initiated at $t = 12$ (illustrated in figure 7.2). Vessel is considered as failed since flaw propagated 90% of the distance through the wall.

Through-Wall Cracking Analysis #2:

This is a different simulation of through-wall cracking behavior of the flaw that initiated in Figure 7.2. The simulation has a progression different from the first simulation because of different sampled values for the cleavage and ductile crack initiation toughness values. This analysis is performed at $t=12$ minutes.

Event 1: Figure 7.4(a) illustrates that the initiated flaw propagates to a depth of 1.77 in. where it arrests since the applied driving force to fracture (K_I) falls below the crack arrest toughness (K_{Ia}).

Event 2: Figure 7.4(b) illustrates that the arrested flaw does not reinitiate in cleavage fracture since the applied driving force to fracture (K_I) does not exceed the cleavage fracture initiation toughness (K_{Ic}). Nor does the flaw reinitiate by ductile tearing since the applied driving force to fracture (K_I) does not exceed the upper shelf crack initiation fracture toughness (K_{Jc}). This flaw has experienced a stable arrest and does not fail the vessel.

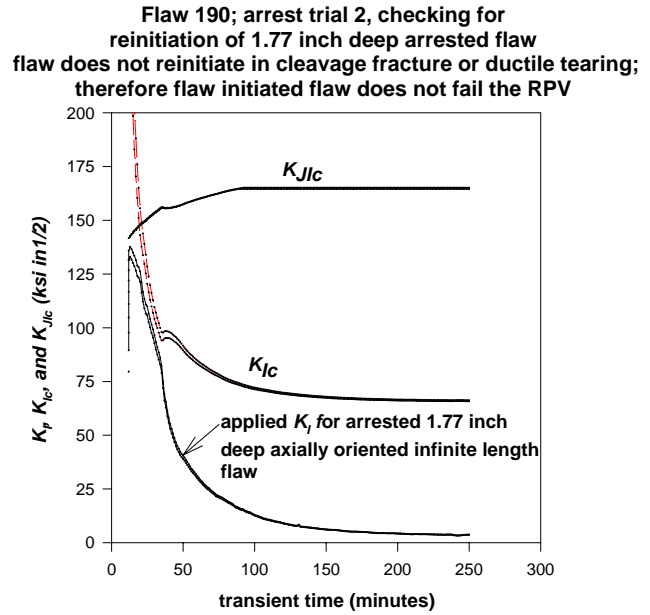
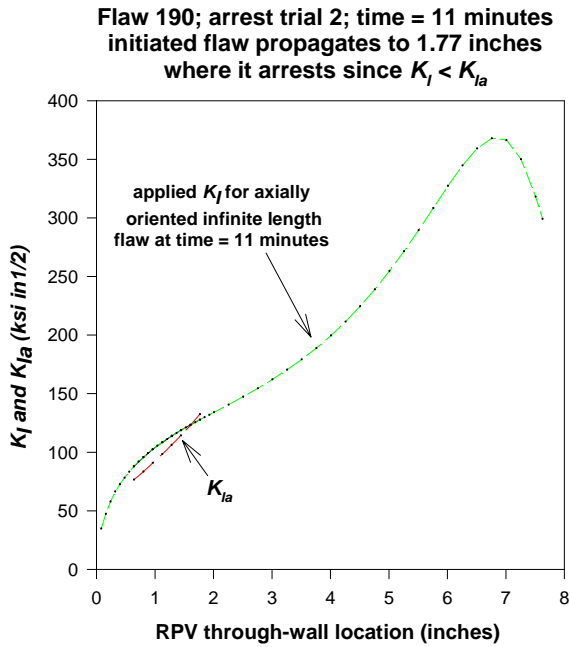


Figure 7.4(a) {left} – Beaver Valley transient sequence 7 – deterministic through-wall analysis for flaw initiated at $t = 11$ (illustrated in figure 7.2) for which case the flaw is arrested at a depth of 1.77 in. since $K_I < K_{Ia}$.

Figure 7.4(b) {right}– Beaver Valley transient sequence 7 – checking for re-initiation of arrested flaw illustrate in 7.4(a). Flaw does not reinitiate in cleavage fracture or ductile tearing.

Deterministic analysis of a simulated flaw subjected to Oconee transient 122 at 60 EFPY

Transient sequence:	Oconee 122	
Transient Description:	Stuck-open pressurizer safety valve that recloses at 6000 seconds (See Figure 122.1 for pressure and temperature variation)	
Flaw Analyzed:	Orientation:	Axial
	Type:	Embedded flaw in weld material
	Depth (2a):	0.604 in
	Length (2c):	0.966 in
	Inner crack tip distance from ID (ℓ):	0.854 in
Embrittlement:	EFPY:	60 years
	Simulated RT_{NDT} at inner crack tip	208°F

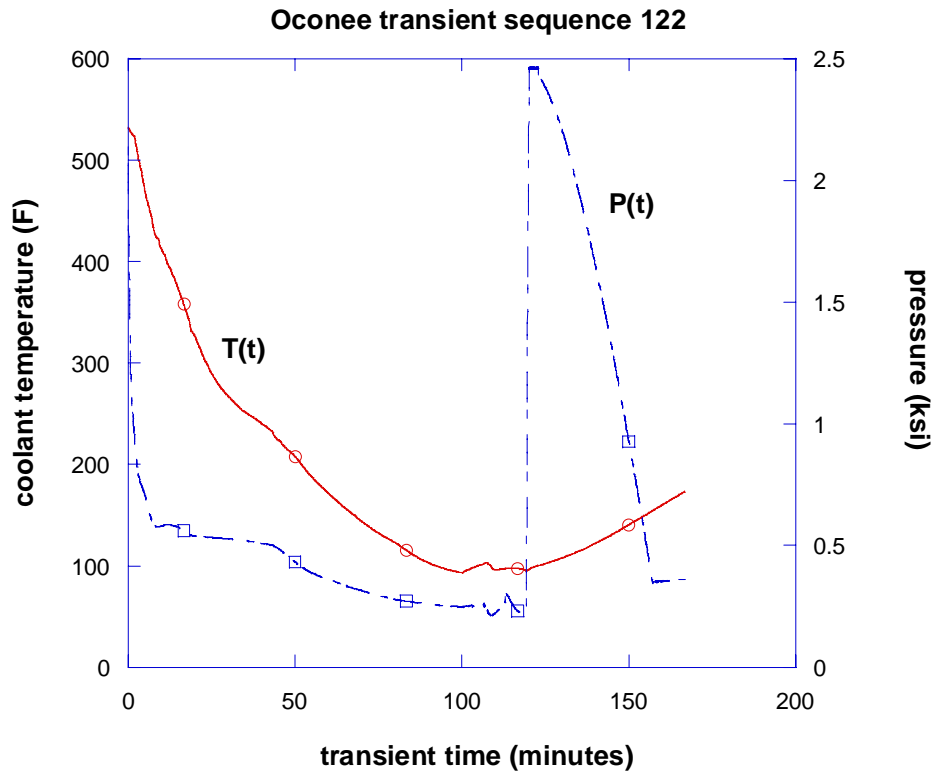


Figure 122.1 Oconee transient 122 – stuck-open pressurizer safety valve that recloses at 6000 seconds.

Crack Initiation

Figure 122.2 illustrates that the conditions for the flaw to have a conditional probability of crack initiation (cpi) > 0 are satisfied: (1) the applied driving force to fracture (K_I) is greater than the minimum of the cleavage fracture initiation toughness (K_{Ic}) distribution (which corresponds to the Weibull ‘a’ parameter), and (2) during the time that applied K_I is greater than the minimum K_{Ic} , the applied K_I must also be

greater than at all previous time steps. The second condition is a necessary condition to overcome effect of warm-prestress.

Figure 122.2 illustrates that the flaw has a conditional probability of initiation (cpi) > 0 in the transient time interval between 119 and 121 minutes. The flaw cannot initiate before a transient time of 120 minutes since this is the first time step at which K_I exceeds the minimum value of K_{Ic} . The flaw cannot initiate after a transient time of 121 minutes because this is the time at which the maximum applied K_I occurs, so warm-prestress prevents crack initiation for all transient times > 121 minutes.

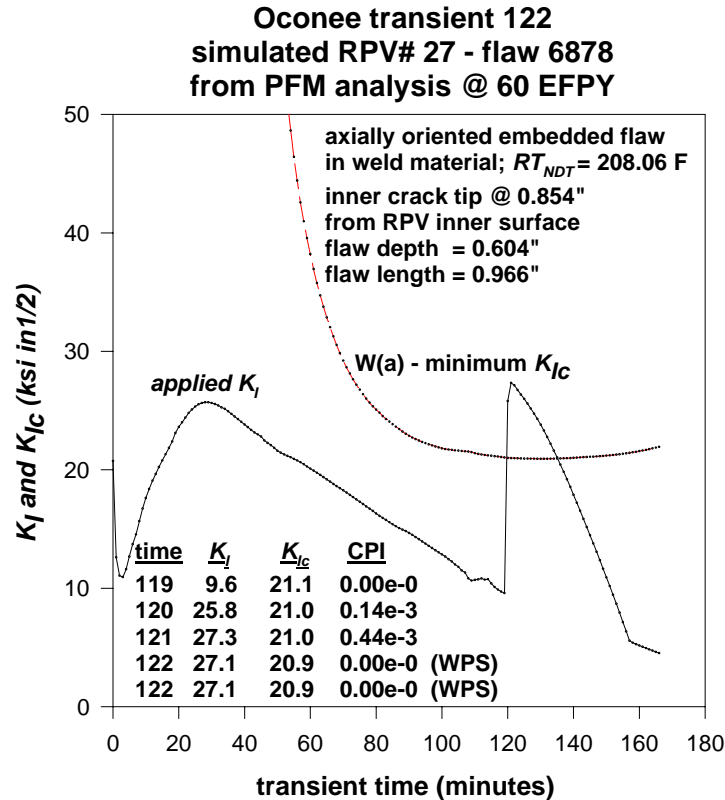


Figure 122.2 – Oconee transient 122 – deterministic LEFM analysis for flaw from PFM Monte Carlo analysis for which $cpi > 0$

Through-Wall Cracking Analysis #1:

This is one simulation of the through-wall cracking behavior of the flaw initiated in Figure 122.2. This analysis occurs at $t=120$ minutes.

Event 1: Figure 122.3 illustrates that the initiated flaw propagates through the wall thickness to failure since the applied driving force (K_I) exceeds the crack arrest toughness (K_{Ia}) through the entire wall thickness at $t=120$ minutes. The mode of failure is plastic instability.

Even though all of the other through-wall analyses performed at this time step have different sampled values for the cleavage and ductile crack initiation toughness values, they all fail due to plastic instability as illustrated in through-wall cracking analysis #1. For Oconee transient 122, all initiated flaws fail; therefore, the conditional probability of through-wall cracking is identical to the conditional probability of crack initiation.

**flaw 6878: arrest trial 1; time = 120 minutes
 initiated flaw propagates to failure by plastic instability**

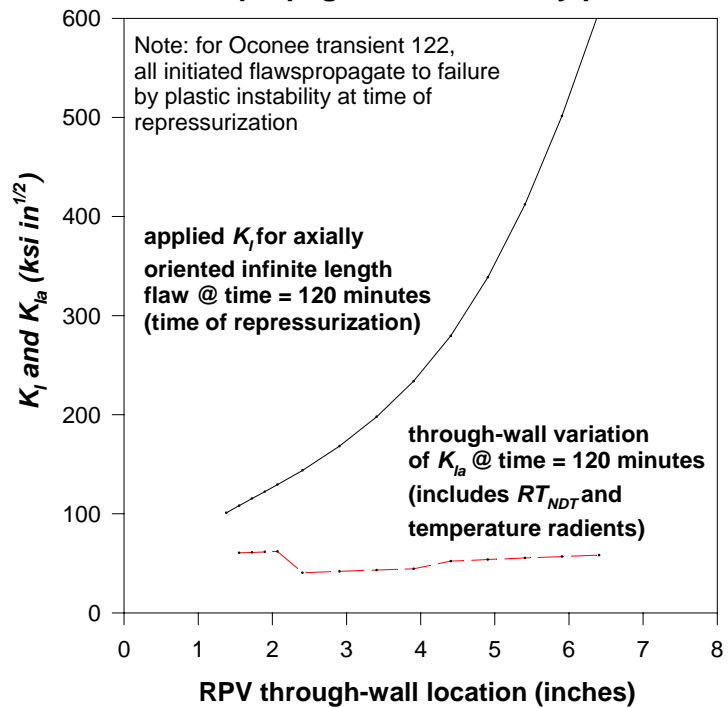


Figure 122.3 – Oconee transient 122 – deterministic through-wall analysis for flaw initiated at t = 120 minutes that results in failure by plastic instability

Deterministic analysis of a simulated flaw subjected to Beaver Valley transient 104 at 60 EFPY

Transient Sequence:	Beaver Valley 104	
Transient Description:	Main Steam Line Break with AFW continuing to feed affected generator for 30 minutes (See Figure 104.1 for pressure and temperature variation).	
Flaw Analyzed:	Orientation:	Circumferential
	Type:	Embedded flaw in weld material
	Depth (2a):	0.321 in
	Length (2c):	0.620 in
	Inner crack tip distance from ID (L):	0.226 in
Embrittlement:	EFPY:	60 years
	Simulated RT_{NDT} at inner crack tip	319°F

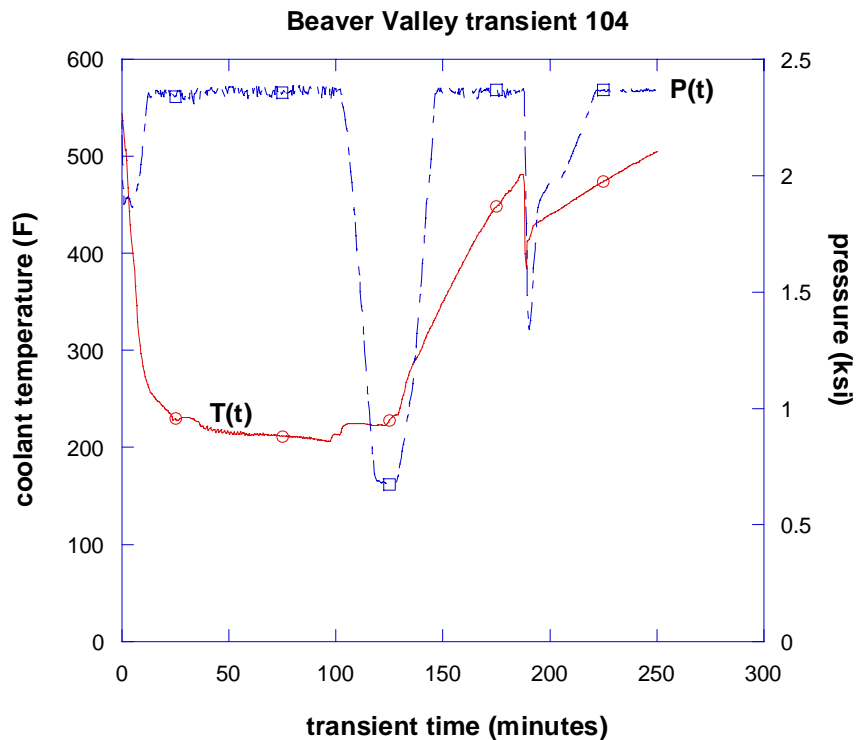


Figure 104.1 Beaver Valley transient sequence 104 – Main Steam Line Break with AFW continuing to feed affected generator for 30 minutes

Crack Initiation

Figure 104.2 illustrates that the conditions for the flaw to have a conditional probability of crack initiation (cpi) > 0 are satisfied: (1) the applied driving force to fracture (K_I) is greater than the minimum of the cleavage fracture initiation toughness (K_{Ic}) distribution (which corresponds to the Weibull ‘a’ parameter), and (2) during the time that applied K_I is greater than the minimum K_{Ic} , the applied K_I must also be greater than at all previous time steps. The second condition is a necessary condition to overcome effect of warm-prestress.

Figure 104.2 illustrates that the flaw has a conditional probability of initiation (cpi) > 0 in the transient time interval between 11 and 12 minutes. The flaw cannot initiate before a transient time of 12 minutes since this is the first time step at which K_I exceeds the minimum value of K_{Ic} . The flaw cannot initiate after a transient time of 12 minutes because this is the time at which the maximum applied K_I occurs, so warm-prestress prevents crack initiation for all transient times > 12 minutes.

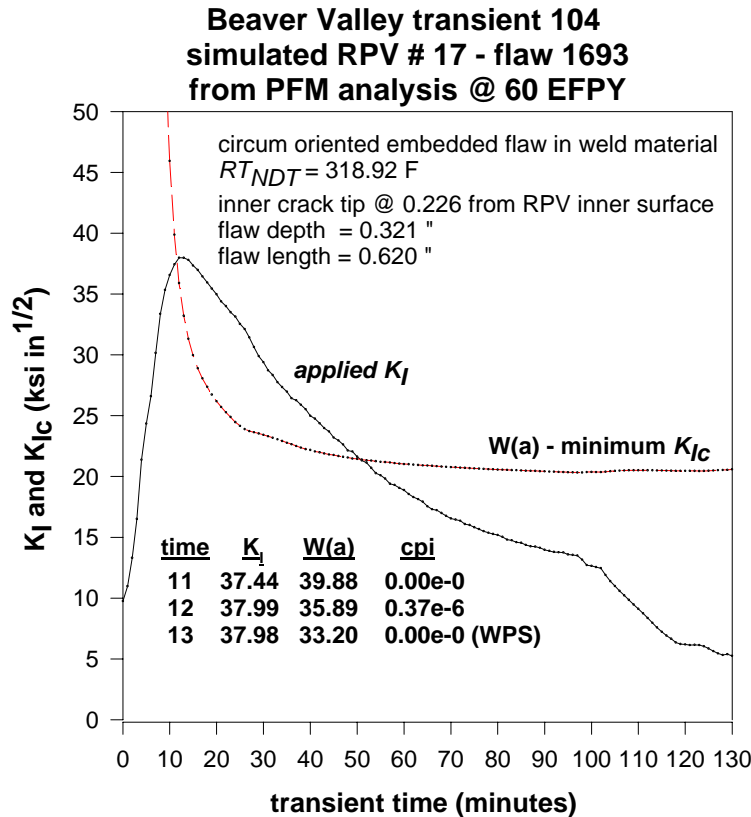


Figure 104.2 Beaver Valley transient sequence 104 – deterministic LEFM analysis of flaw from PFM Monte Carlo analysis for which $cpi > 0$

Through-Wall Cracking Analysis #1:

This is one simulation of the through-wall cracking behavior of the flaw initiated in Figure 104.2. This analysis begins at $t=12$ minutes.

Event 1: Figure 104.3(a) illustrates that the initiated flaw propagates to a depth of 1.93-in. where it arrests since the applied driving force to fracture (K_I) for the 360 degree continuous circumferential flaw falls below the crack arrest toughness (K_{Ia}).

Event 2: Figure 104.3(b) illustrates that the flaw arrested in figure 104.3(a) reinitiates at $t=13$ minutes by ductile tearing since the applied driving force to fracture (K_I) for the 360 degree continuous circumferential flaw is greater than the upper shelf crack initiation fracture toughness (K_{Ic}).

Event 3: Figure 104.3(c) illustrates that the flaw reinitiated by ductile tearing propagates by cleavage (since $K_I > K_{Ia}$) to a depth of 6.09 in. where it arrests since $K_I < K_{Ia}$. The FAVOR model allows a flaw that reinitiates by a stable ductile tear (of some finite distance) to resume cleavage fracture propagation if $K_I > K_{Ia}$. This is consistent with observations in large-scale fracture experiments [TSE REFS].

Event 4: Figure 104.3(d) illustrates that at t=14 minutes, the arrested flaw reinitiates in unstable ductile tearing; which propagates through the vessel wall, failing the vessel.

**simulated RPV 17; flaw 1693; arrest trial 56; time = 12 minutes
initiated flaw propagates to 1.929 inches
where its arrests since $K_I < K_{Ia}$**

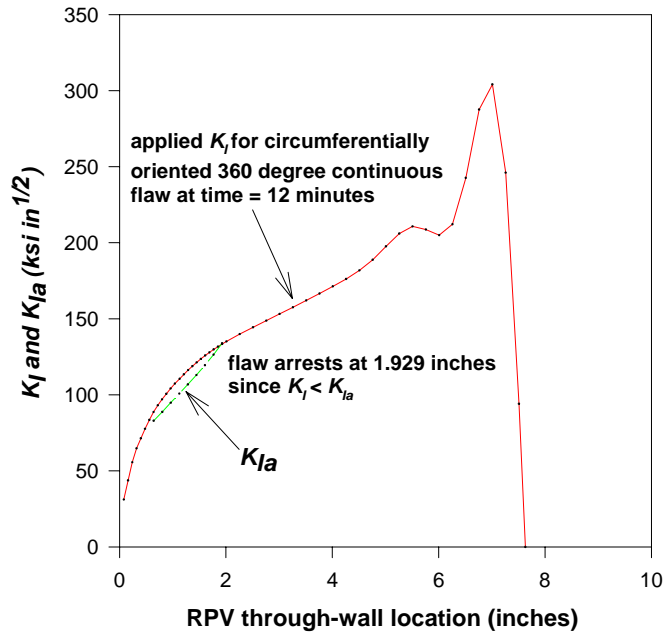
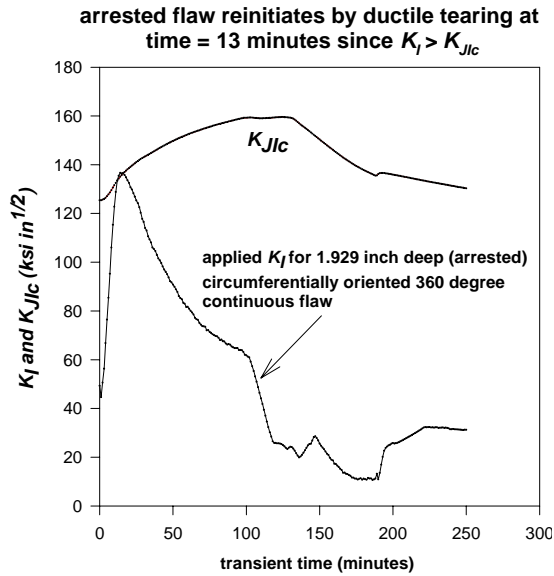


Figure 104.3(a) Beaver Valley transient sequence 104 – deterministic through-wall analysis for flaw initiated at t = 12 minutes (illustrated in figure 104.2) for which case the flaw is arrested since the applied driving force to fracture (K_I) falls below the crack arrest toughness (K_{Ia}).

simulated RPV 17; flaw 1693; arrest trial 56
time histories of applied K_I and K_{JIC} at tip of
arrested flaw



flaw 190; arrest trial 56; time = 13 minutes
after reinitiation of arrested flaw by ductile tearing
flaw propagates to 6.09 inches where it arrests since $K_I < K_{Ia}$

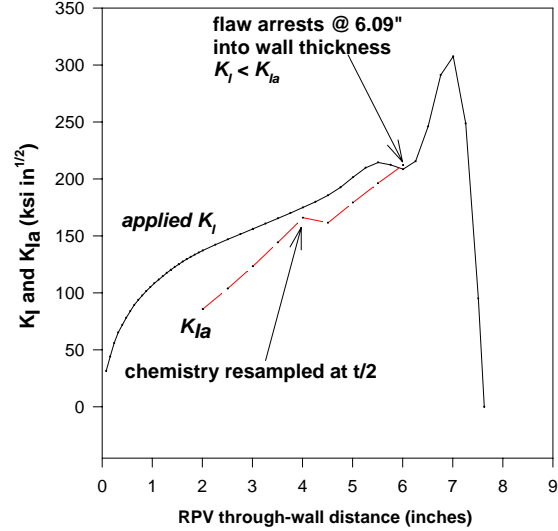


Figure 104.3(b) {left} Beaver Valley transient sequence 104 – deterministic analysis for arrested flaw illustrated in figure 104.3(a). Arrested flaw reinitiates by ductile tearing at time = 13 minutes since $K_I > K_{JIC}$.

Figure 104.3(c) {right} Beaver Valley transient sequence 104 – after re-initiation of arrested flaw by ductile tearing, flaw propagates to 6.09 in. where it arrests since $K_I < K_{Ia}$

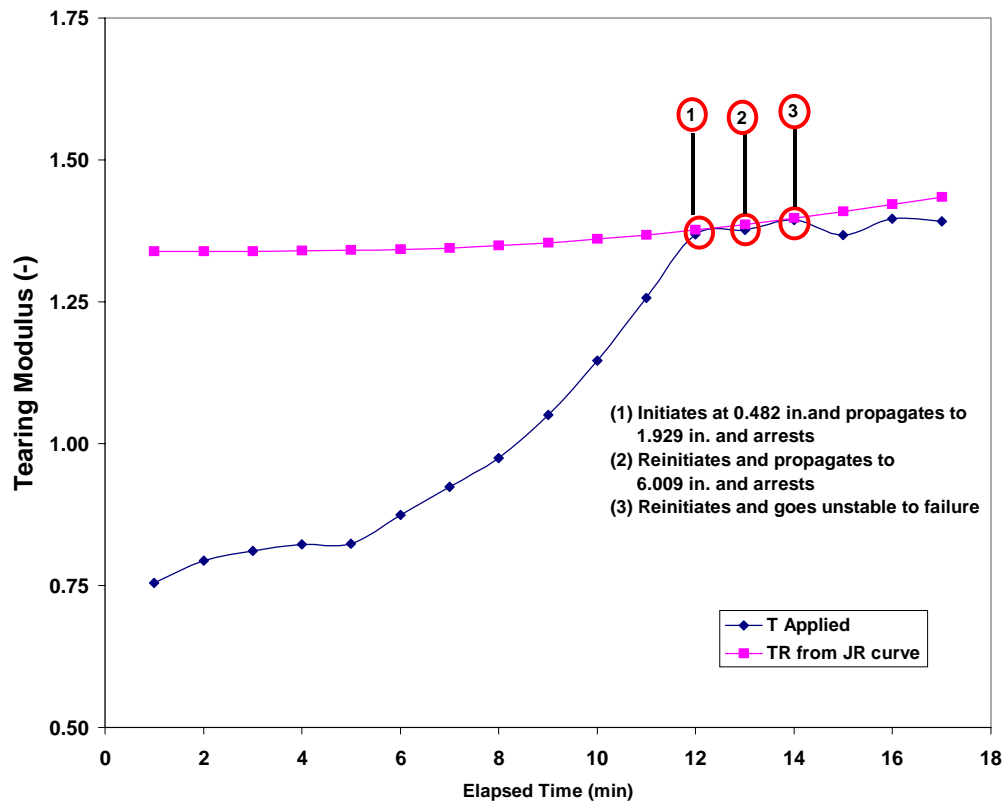


Figure 104.3(d) Beaver Valley transient sequence 104 –at time = 14 minutes, the 6.09 in. deep arrested flaw (illustrated in figure 104.3(c)) reinitiates in unstable ductile tearing to failure.

Through-Wall Cracking Analysis #2:

This is a different simulation of through-wall cracking behavior of the flaw that initiated in Figure 104.2. The simulation has a progression different from the first simulation because of different sampled values for the cleavage and ductile crack initiation toughness values. This analysis is performed at t=12 minutes.

Event 1: Figure 104.4(a) illustrates that the initiated flaw propagates to a depth of 1.92-in. where it arrests since the applied driving force to fracture (K_I) falls below the crack arrest toughness (K_{Ia}).

Event 2: Figure 104.4(b) illustrates that the arrested flaw does not reinitiate in cleavage fracture since the applied driving force to fracture (K_I) does not exceed cleavage fracture initiation toughness (K_{Ic}). Nor does the flaw reinitiate by ductile tearing since the applied driving force to fracture (K_I) does not exceed the upper shelf crack initiation fracture toughness (K_{Jc}). Therefore, this flaw has experienced a stable arrest and does not fail the vessel.

simulated RPV 17; flaw 1693, arrest trial 7; time = 12 minutes
 initiated flaw propagates to 1.929 inches
 where its arrests since $K_I < K_{Ia}$

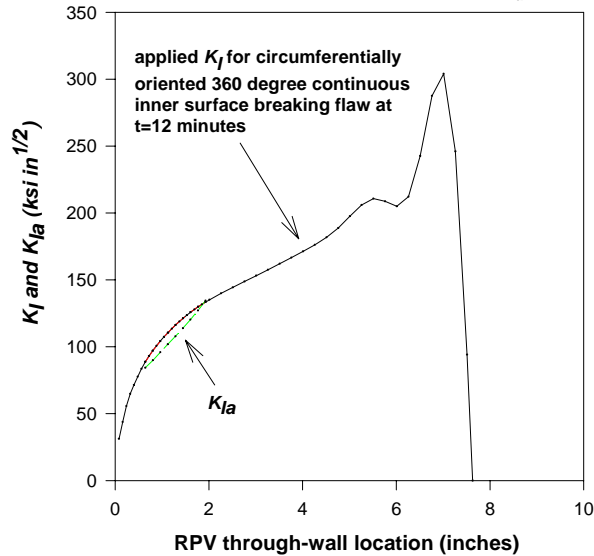


Figure 104.4(a) Beaver Valley transient sequence 104 – deterministic through-wall analysis for flaw initiated at $t = 12$ minutes (illustrated in figure 104.2) for which case the flaw is arrested.

Beaver Valley transient 104; flaw 1693; arrest trial 7
 checking for re-initiation of arrested flaw beginning @ $t = 13$ min

cleavage: $K_I < K_{Ic} \implies$ no cleavage re-initiation

ductile: $K_I < K_{Jlc} \implies$ no ductile re-initiation

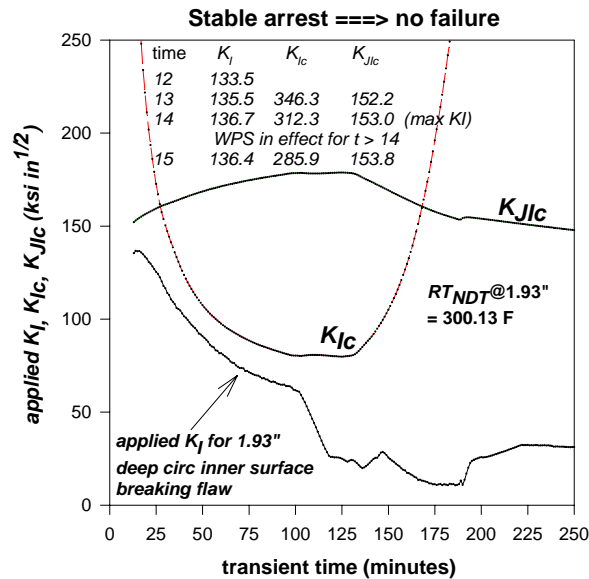


Figure 104.4(b) Beaver Valley transient sequence 104 – checking for re-initiation of arrested flaw illustrated in figure 104.4 (a). Flaw does not reinitiate in cleavage fracture or ductile tearing; therefore initiated flaw does not propagate to failure.

Deterministic analysis of a simulated flaw subjected Palisades transient 55 at 60 EFPY

Transient sequence:	Palisades transient 55	
Transient Description:	Turbine/reactor trip with two stuck-open valves combined with controller failure (See Figure 55.1 for pressure and temperature variation)	
Flaw Analyzed:	Orientation:	Axial
	Type:	Embedded flaw in weld material
	Depth (2a):	0.263 in
	Length (2c):	0.928 in
	Inner crack tip distance from ID (ℓ):	0.342 in
Embrittlement:	EFPY:	60 years
	Simulated RT_{NDT} at inner crack tip	390°F

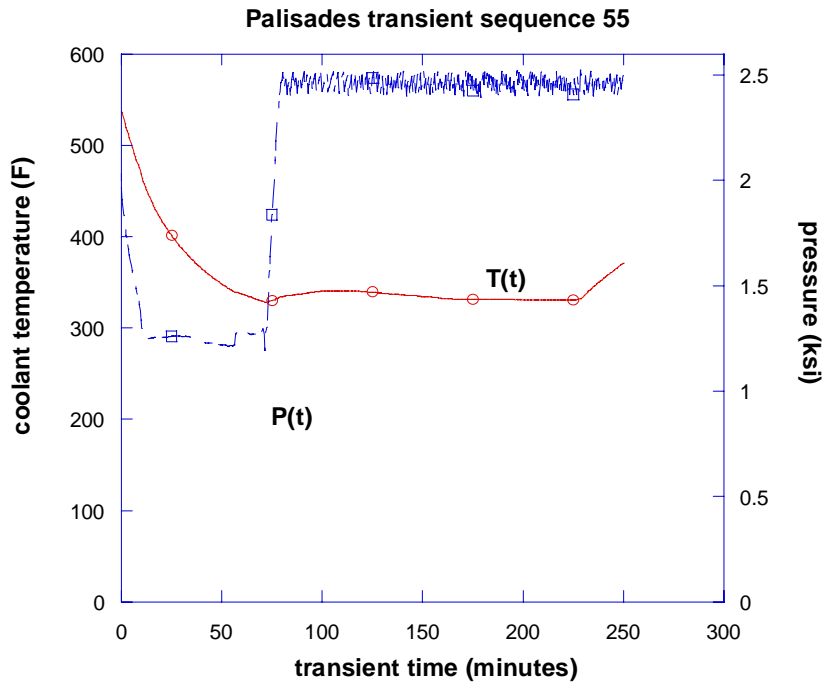


Figure 55-1 Palisades transient sequence 55 that results from a turbine/reactor trip with two stuck-open valves combined with controller failure.

Crack Initiation

Figure 55.2 illustrates that the conditions for the flaw to have a conditional probability of crack initiation (cpi) > 0 are satisfied: (1) the applied driving force to fracture (K_I) is greater than the minimum of the cleavage fracture initiation toughness (K_{Ic}) distribution (which corresponds to the Weibull ‘a’ parameter), and (2) during the time that applied K_I is greater than the minimum K_{Ic} , the applied K_I must also be greater than at all previous time steps. The second condition is a necessary condition to overcome effect of warm-prestress.

Figure 55.2 illustrates that the flaw has a conditional probability of initiation (cpi) > 0 in the transient time interval between 78 and 80 minutes. The flaw cannot initiate before a transient time of 78 minutes since this is the first time step at which K_I exceeds the minimum value of K_{Ic} . The flaw cannot initiate after a transient time of 80 minutes because this is the time at which the maximum applied K_I occurs, so warm-prestress prevents crack initiation for all transient times > 80 minutes.

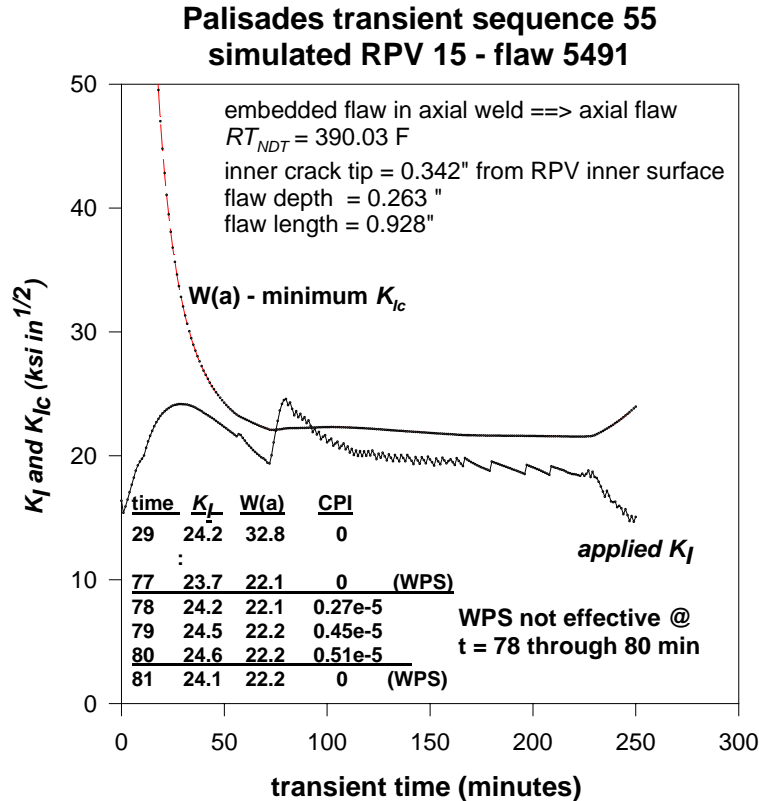


Figure 55-2 Palisades transient sequence 55 – deterministic LEFM analysis for flaw from PFM Monte Carlo analysis for which $cpi > 0$

Through-Wall Cracking Analysis #1:

This is one simulation of the through-wall cracking behavior of the flaw initiated in Figure 55.2. This analysis occurs at $t=78$ minutes.

Event 1: Figure 55.3 illustrates a deterministic through-wall analysis at time = 78 minutes in which the initiated flaw propagates through the wall, since the applied driving force to fracture (K_I) exceeds the crack arrest toughness (K_{Ia}), to a depth such that the failure is by plastic instability. It should be noted that in this case failure by plastic instability occurred at a more shallow depth that propagation to 90% of the wall thickness. Had the failure not occurred by plastic instability, from figure 55.3, it is clear that flaw would have propagated to 90% of the wall thickness in cleavage and therefore would have been considered as failed. Failure by plastic instability is a common mode of failure associated with transients that have repressurizations.

**Flaw 5491; arrest trial 1; time = 78 minutes
initiated flaw propagates without arrest to failure
by plastic instability**

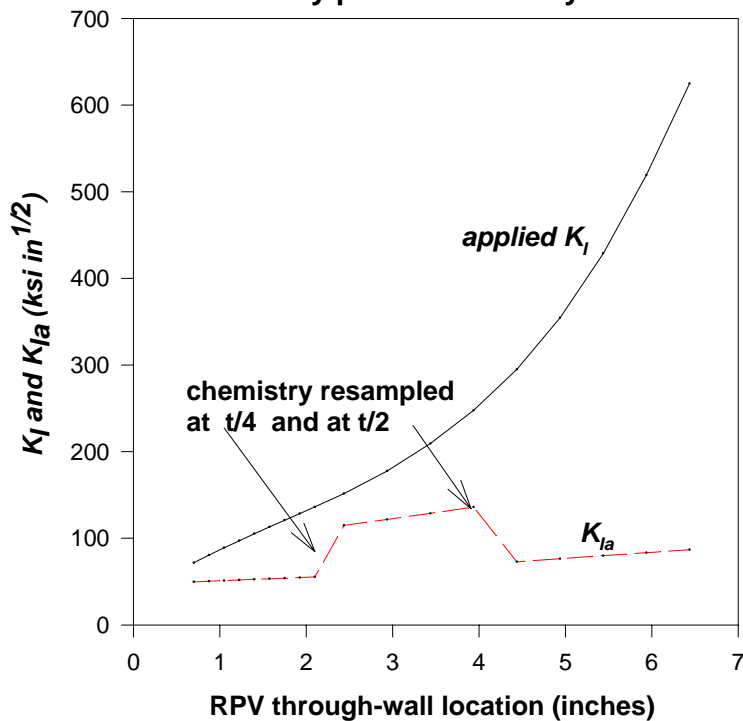


Figure 55-3 Palisades transient sequence 55 – deterministic through-wall analysis for flaw initiated at 78 minutes that propagates through the wall without arrest resulting in failure by plastic instability.

Through-Wall Cracking Analysis #2:

This is a different simulation of through-wall cracking behavior of the flaw that initiated in Figure 55.2. The simulation has a progression different from the first simulation because of different sampled values for the cleavage and ductile crack initiation toughness values. This analysis is also performed at t=78 minutes.

Event 1: Figure 55.4(a) illustrates that the initiated flaw propagates to a depth of 2.44 in. where it arrests since the applied driving force to fracture (K_I) falls below the crack arrest toughness (K_{IIa}). Note that the discontinuity in crack arrest toughness is due to a re-sampling of chemistry, which is performed at t/4, t/2, and 3t/4 through-wall locations for weld material.

Event 2: Figure 54.4(b) illustrates that the flaw arrested in figure 55.4(a) reinitiates at t=79 minutes by ductile tearing since the applied driving force to fracture (K_I) for the infinite length inner-surface breaking axially oriented flaw is greater than the upper shelf crack initiation fracture toughness (K_{IIc}) and that the applied K_I for the 2.44 in. deep flaw is greater than at previous time steps.

Event 3: Figure 54.4(c) illustrates that the flaw reinitiated by ductile tearing propagates by cleavage (since $K_I > K_{IIa}$) at time=79 minutes to a depth of 2.69 in. where it arrests since $K_I < K_{IIa}$.

Event 4: Figure 54.4(d) illustrates checking for re-initiation of the arrested flaw beginning a time=80 minutes. The arrested flaw does not reinitiate in cleavage fracture since the applied driving force to fracture (K_I) does not exceed cleavage fracture initiation toughness (K_{Ic}). Nor does the flaw reinitiate by ductile tearing, even though the applied driving force to fracture (K_I) does exceed the upper shelf crack initiation fracture toughness (K_{Jlc}), however, at times after the maximum value of the applied driving force to fracture (K_I), therefore, warm prestress inhibits re-initiation by ductile tearing.

**Flaw 5491; arrest trial 28; time=78
initiated flaw propagates to 2.44 inches
where it arrests since $K_I < K_{Ia}$**

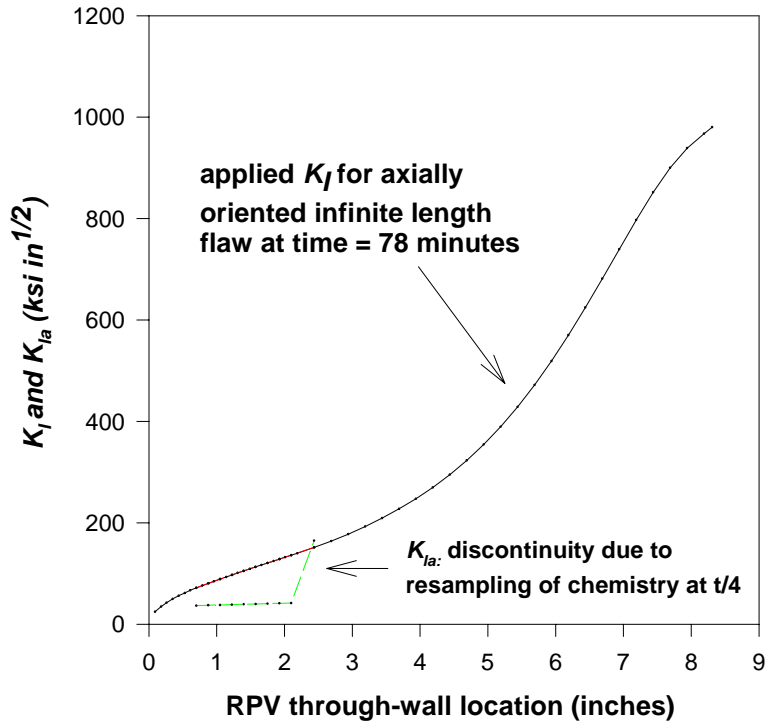


Figure 55-4(a) Palisades transient sequence 55 – deterministic through-wall analysis for flaw initiated at 78 minutes (illustrated in figure 55-2) that propagates to 2.44 where it arrest since $K_I < K_{Ia}$. The discontinuity in K_{Ia} is due to re-sampling of chemistry at $t/4$.

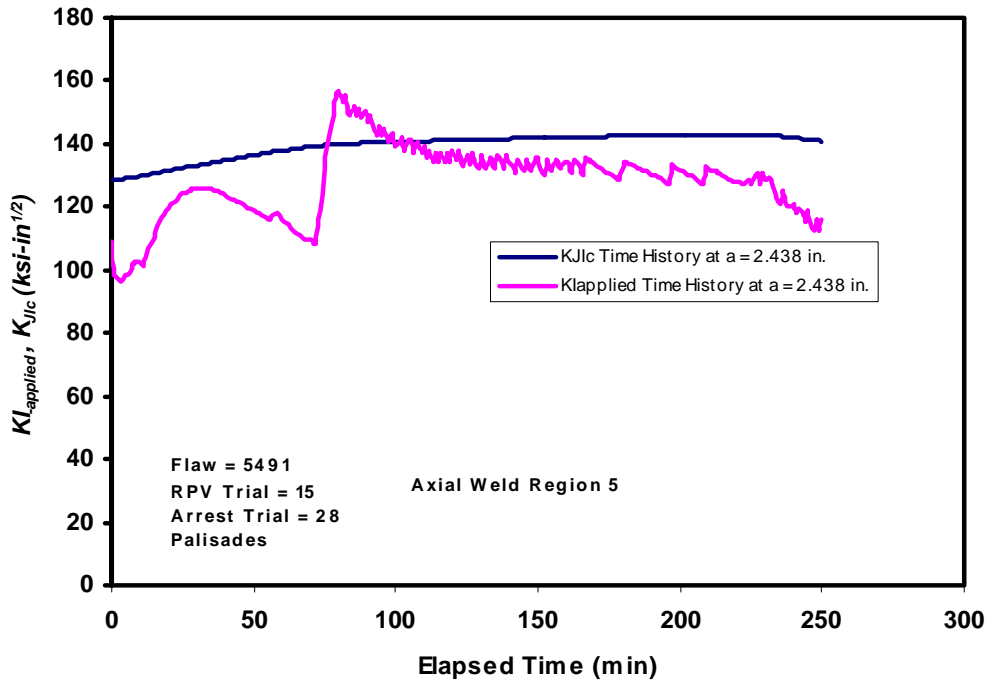


Figure 55-4(b) Palisades transient sequence 55 – arrested flaw illustrated in figure 55-4(a) reinitiates in ductile tearing at time = 79 since $K_I > K_{Ic}$

Flaw 5491; arrest trial 28; time = 79 minutes
 reinitiated flaw propagates to depth of 2.69
 where it arrests since $K_I < K_{Ia}$

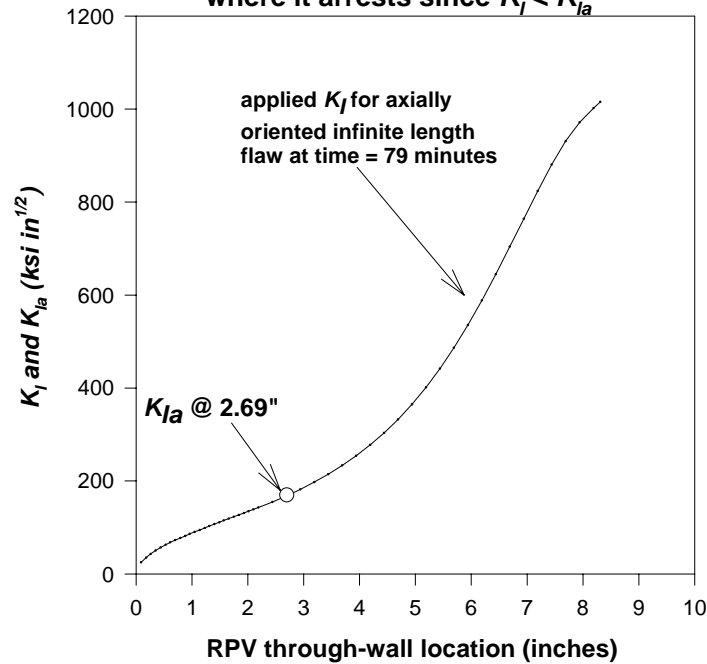


Figure 55-4(c) Palisades transient sequence 55 – 2.44 in. flaw that reinitiated in ductile tearing propagates to depth 2.69 in where it arrests since $K_I < K_{Ia}$

flaw 5491; arrest trial 28; checking for reinitiation of arrested
 flaw beginning at time = 80 minutes
 $K_I > K_{JIC}$; however, K_I is lower than previous
 maximum value for K_I for arrested flaw; therefore, WPS is effective

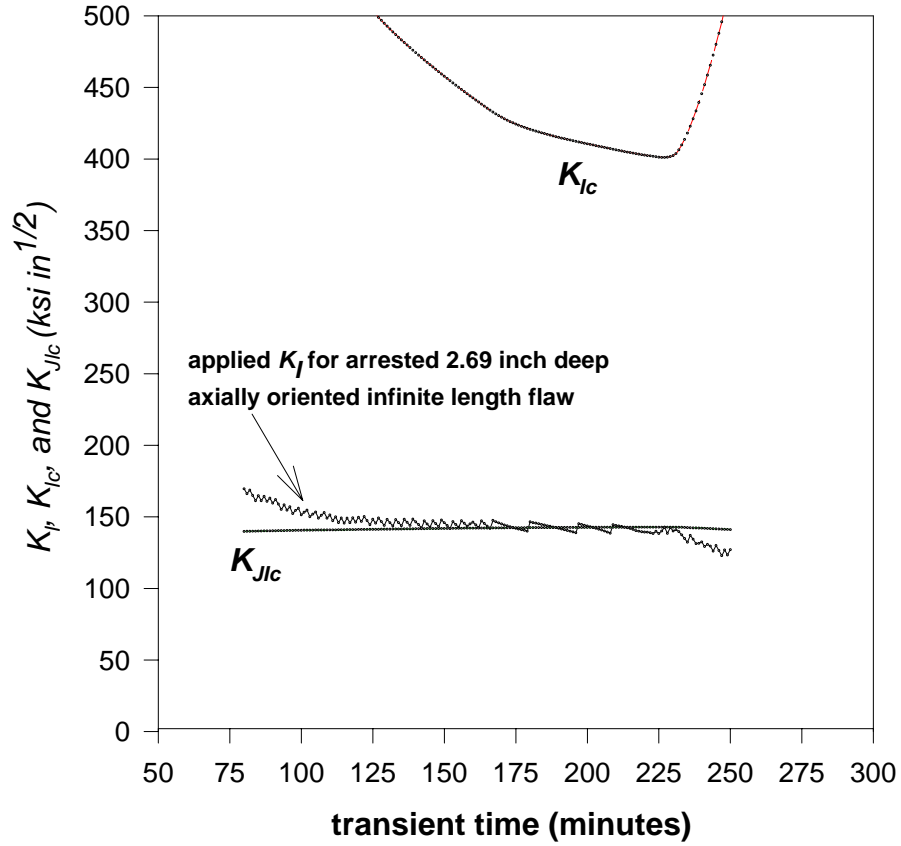


Figure 55-4(d) Palisades transient sequence 55 –checking for re-initiation of arrested flaw illustrated in figure 55-4(c). Flaw does not reinitiate in cleavage fracture ($K_I < K_{Ic}$) or ductile tearing. $K_I > K_{JIC}$; however, at times later than the maximum K_I occurred for arrested flaw; therefore WPS inhibits re-initiation by ductile tearing.

Appendix G – Flaw Distributions for Forgings

This Appendix includes two articles prepared by Dr. Frederic Simonen of the Pacific Northwest National Laboratory concerning flaw distributions in forgings. The staff used these articles as the basis of the forging flaw sensitivity studies reported in Section 9.2.2.2.

Technical Basis for the Input Files to FAVOR Code for Flaws in Vessel Forgings

F.A. Simonen
Pacific Northwest National Laboratory
Richland, Washington

July 28, 2004

Pacific Northwest National Laboratory (PNNL) has been funded by the U.S. Nuclear Regulatory Commission (NRC) to generate data on fabrication flaws that exist in reactor pressure vessels (RPV). Work has focused on flaws in welds but with some attention also to flaws in the base metal regions. Data from vessel examinations along with insights from an expert judgment elicitation (MEB-00-01) and from applications of the PRODIGAL flaw simulation model (NUREG/CR-5505, Chapman et. al. 1998) have been used to generate input files (see report NUREG/CR-6817, Simonen et. al. 2003) for probabilistic fracture mechanics calculations performed with the FAVOR code by Oak Ridge National Laboratory. NUREG/CR-6817 addresses only flaws in plate materials and provided no guidance for estimating the numbers and sizes of flaws in forging materials. More recent studies have examined forging material, which has provided a data on flaws that were detected and sized in the examined material. At the request of NRC staff PNNL has used these more recent data to supplement insights from the expert judgment elicitation to generate FAVOR code input files for forging flaws. The discussion below describes the technical basis and results for the forging flaw model.

Nature of Base Metal Flaws

PNNL examined material from some forging material from a Midland vessel as described by Schuster (2002). The forging was made during 1969 by Ladish. Examined material included only part of the forging that had been removed from the top of the forged ring as scrap not intended for the vessel. This material was expected to have more than the average flaw density, and as such may contribute to the conservatism of any derived flaw distribution.

Figures 1 and 2 show micrographs of small flaws in plate and forging materials. These flaws are inclusions rather than porosity or voids. They are also not are planer cracks. Therefore their categorization as simple planar or as volumetric flaws is subject to judgment. The plate flaw of Figure 1 has many sharp and crack-like features, whereas such features are not readily identified for the particular forging flaw seen in Figure 2. It should, however, be emphasized that the PNNL examined only a limited volume of both plate and forging material and found very few flaws in examined material. It is not

possible to generalize from such a small sample of flaws. Accordingly, the flaw model makes assumptions that may be somewhat conservative, due to the limited data on the flaw characteristics.

Flaw Model for Forging Flaws

The model for generating distributions of forging flaws for the FAVOR code uses the same approach as that for modeling plate flaws as described in NUREG/CR-6817. The quantitative results of the expert elicitation are used along with available data from observed forging flaws. The flaw data were used as a “sanity check” on the results of the expert elicitation. Figure 3 summarizes results of the expert elicitation. Each expert was asked to estimate ratios between flaw densities in base metal compared to the corresponding flaw densities observed in the weld metal of the PVRUF vessel. Separate ratios were requested for plate material and forging material.

As indicated in Figure 3, the parameters for forging flaws are similar to those for plate flaws. The forging and plate models used the same factor of 0.1 for the density of “small” flaws (flaws with through-wall dimensions less than the weld bead size of the PVRUF vessel). The density of “large” flaws in forging material is somewhat greater than the density of flaws in plate material. The factor of 0.025 for the flaw density is replaced by a factor of 0.07 for forging flaws. A truncation level of 0.11 mm is used for both plate and forging flaws. As described in the next section the data from forging examinations show that these factors are consistent with the available data. It is noted that the assumption for the 0.07 factor is supported by only a single data point corresponding to the largest observed forging flaw (with a depth dimension of 4 mm).

The factors of 0.1 and 0.07 came from the recommendations from the expert elicitation on vessel flaws. As noted below the very limited data from PNNL’s examinations of forging material show that these factors are consistent with the data, although the 0.07 factor is supported by only one data point for an observed forging flaw with a 4-mm depth dimension.

Comparison with Data on Observed Flaws

The PNNL examinations of vessel materials included both plate materials and forging materials. For plate flaws less than 4-mm in through-wall depth dimension, Figure 4 shows data from NUREG/CR-6817 that shows frequencies for plate flaws. Also shown for comparison are the flaw frequencies for the welds of the PVRUF and Shoreham vessels. This plot confirmed results of the expert judgment elicitation (Figure 4) and indicated: 1) there are fewer flaws in plate material than in weld material, and 2) there is about a 10:1 difference in flaw frequencies for plates versus welds.

PNNL generated the data on flaws in forgings after preparation of NUREG/CR-6817. Forging data are presented in Figures 5 and 6 along with the previous data for flaws in the PVRUF plate material. There is qualitative agreement with the results of the expert judgment elicitation (Figure 4), which indicates that 1) plate and forging materials have similar frequencies for small (2 mm) flaws, and 2) forging material have higher flaw frequencies for larger (>4 mm) flaws.

Inputs for FAVOR Code

Figure 7 compares the flaw frequencies for plates and forgings that were provided to ORNL as input files for the FAVOR code. This plot shows mean frequencies from an uncertainty distribution as described by the flaw input files. It is seen that the curves for plate and forging flaws are identical for small flaws but show differences for the flaws larger than 3% of the vessel wall thickness. Also seen is the effect of truncating the flaw distribution at a depth of 11 mm (about 5% of the wall thickness).

References

Jackson, D.A. and L. Abramson, 2000. *Report on the Preliminary Results of the Expert Judgment Process for the Development of a Methodology for a Generalized Flaw Size and Density Distribution for Domestic Reactor Pressure Vessel*, MED-00-01, PRAB-00-01, U.S. Nuclear Regulatory Commission.

Schuster, G.J., 2002. "Technical Letter Report – JCN-Y6604 – Validated Flaw Density and Distribution Within Reactor Pressure Vessel Base Metal Forged Rings," prepared by Pacific Northwest National Laboratory for U.S. Nuclear Regulatory Commission, December 20, 2002.

Simonen, F.A., S.R. Doctor, G.J. Schuster and P.G. Heasler, 2003. *A Generalized Procedure for Generating Flaw-Related Inputs for the FAVOR Code*, NUREG/CR-6817, Rev. 1, prepared by Pacific Northwest National Laboratory for U.S. Nuclear Regulatory Commission.



Figure 1 Small Flaw in Plate Material

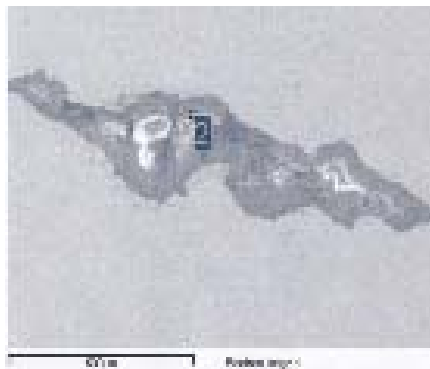
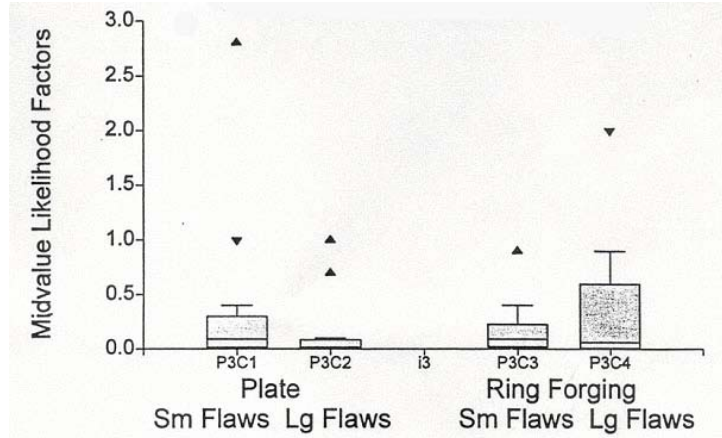


Figure 2 Small Flaw in Forging Material



Base Metal vs. Weldmetal				
	Plate vs. Welds		Ring Forgings vs. Welds	
	Small Flaws	Large Flaws	Small Flaws	Large Flaws
MIN	.0004	.001	.001	.002
LQ	.015	.01	.02	.007
MED	.1	.025	.1	.07
UQ	.3	.09	.2	.6
MAX	12.0	1.0	.9	2.0

Figure 3 Relative Flaw Densities of Base Metal Compared to Weld Metal as Estimated by Expert Judgment Process (from Jackson and Abramson 2000)

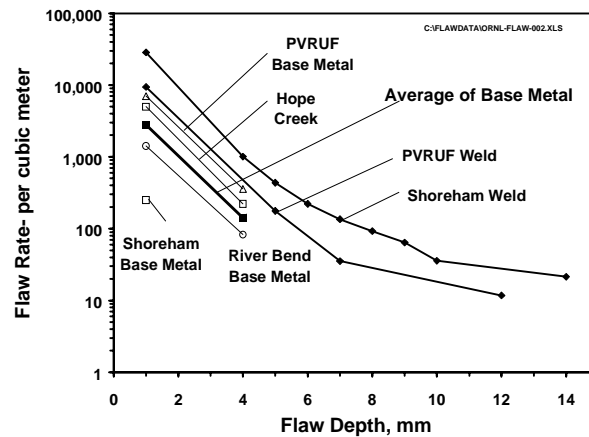


Figure 4. Flaw Frequencies for Plate Materials with Comparisons to Data for Weld Flaws

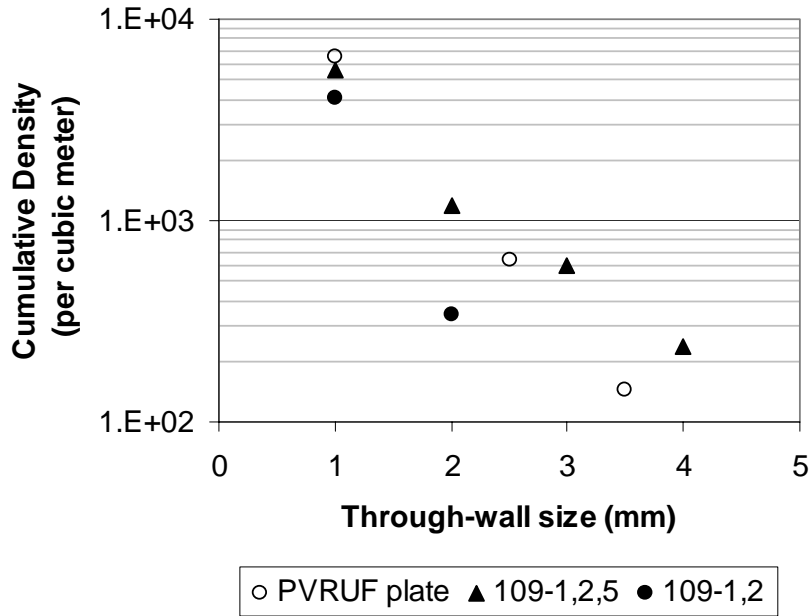


Figure 5. Validated Flaw Density and Size Distribution for Three Forging Specimens. Cumulative flaw density is the number of flaws per cubic meter of equal or greater size.

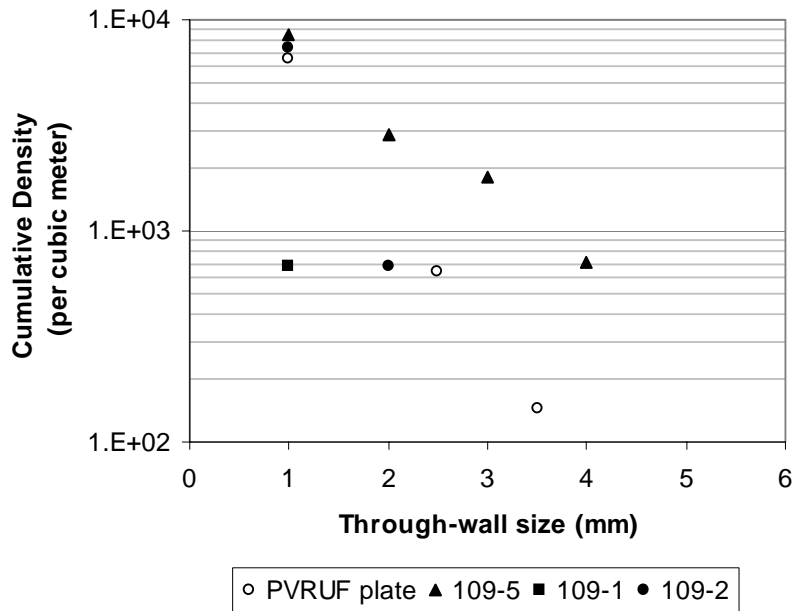


Figure 6 Average of Validated Cumulative Flaw Density for Forging Material, A508

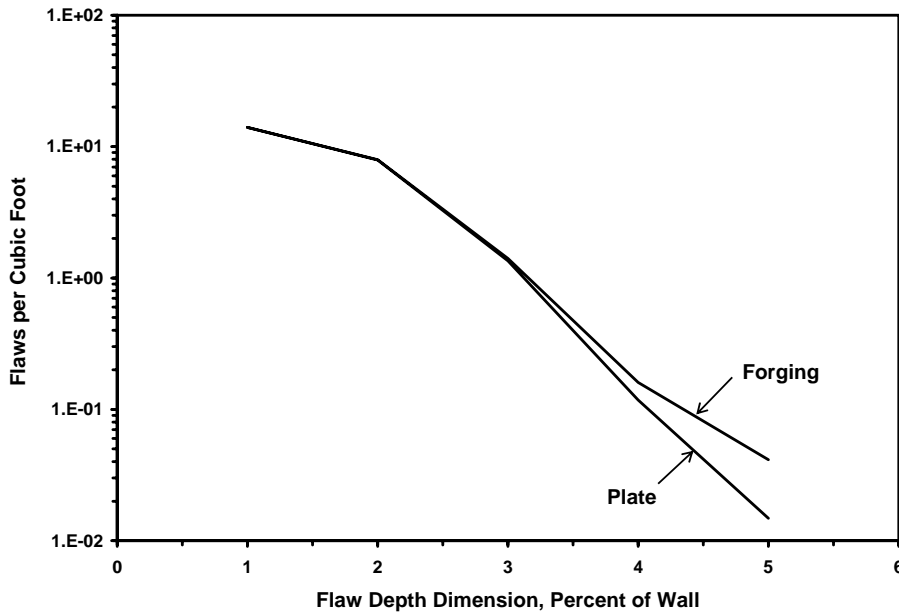


Figure 7 Comparison of Flaw Distributions for Forging and Plate

Basis for Assigning Subclad Flaw Distributions

F.A. Simonen
 Pacific Northwest National Laboratory
 Richland, Washington

September 29, 2004

Pacific Northwest National Laboratory (PNNL) has supported the U.S. Nuclear Regulatory Commission (USNRC) in the efforts to revise the Pressurized Thermal Shock (PTS) Rule. In this role PNNL has provided Oak Ridge National Laboratory (ORNL) with inputs to describe the distributions of fabrication flaws in reactor pressure vessels. These inputs, consisting of computer files, have been a key input to the probabilistic fracture mechanics code FAVOR. Flaw inputs have addressed seam welds, cladding and base metal materials, but had specifically excluded subclad flaws associated with the heat affected zone (HAZ) from the process that deposits stainless steel cladding to the inner surface of the vessel. Recently ORNL was requested by USNRS to evaluate the potential contribution of these subclad flaws to reactor pressure vessel failure for PTS conditions. The present paper describes the technical basis for the subclad flaw input files that PNNL provided to ORNL for use with the FAVOR code.

PNNL has examined material from vessels welds, basemetal and cladding and has used the data on observed flaws in these material types to establish statistical distributions for the numbers and sizes of flaws in these categories of materials. None of the examined material showed any evidence of the type of subclad flaws of interest. Therefore, the numbers and sizes of sub clad flaws for a vessel susceptible to such cracking was estimating from a review of the literature. The primary source was a comprehensive paper summarizing European work from the 1970's (A. Dhooge, R.E. Dolby, J. Seville, R. Steinmetz ad A.G. Vinckier, "A Review of Work Related to Reheat Cracking in Nuclear Reactor Pressure Vessel Steels", International Journal of Pressure Vessels and Piping, Vol. 6, 1978, pp.329-409). This paper was based on experience with vessel cracking in Europe and subsequent research programs conducted during the 1970's. The paper should therefore be relevant to US concerns with older vessels that may have been fabricated with European practices.

The literature shows that subclad cracks 1) are shallow flaws extending into the vessel wall from the clad-to-basemetal interface with 4-mm being cited as a bounding through-wall depth dimension, 2) have orientations normal to the direction of welding for clad deposition - giving axial cracks in a vessel beltline, 3) occur as dense arrays of small cracks extending into the vessel wall from the clad to basemetal interface, 4) extend to depths limited by the heat affected zone. Pictures in the cited paper show networks of cracks with typical depths estimated from micrograph being significantly less than the bounding 4-mm depth. The cracks occur perpendicular to the direction of welding and are clustered where the passes of strip clad contact each other. Subclad flaws are much more likely to occur in particular grades of pressure vessel steels that have chemical compositions that enhance the likelihood of cracking. Forging grades such as A508 are more susceptible than plate materials such as A533. High levels of heat input during the cladding process also enhance the likelihood of subclad cracking. In addition other details of the cladding process are important such as single layer versus two layer cladding.

The numbers of cracks per unit area of vessel inner surface were estimated from Figure 1 of the Dhooge paper. Cracking was shown to occur in bands estimated to have a width of 4 mm. This dimension was used to estimate a bounding length of subclad cracks. The longest individual cracks in Figure 1 were about 2-mm versus the 4-mm width dimension of the zone of cracking. By counting the number of cracks pictured in small region of vessel surface crack density of 80,512 flaws per square meter was estimated.

The flaw input files as provide to ORNL were based on the following assumptions:

- (1) The crack depth dimensions were described by a uniform statistical distribution from 0 to 2 mm with no cracks greater than 2 mm in depth.
- (2) The crack lengths were also described by a uniform statistical distribution. Like our assumption for flaws in seam welds, the amount by which flaw lengths exceed their corresponding depth dimension is taken to be a uniform distribution from 0 to 4 mm.
- (3) The flaw density expressed as flaws per unit area was converted (for purposes of the FAVOR code) to flaws per unit volume based on the total volume of the metal in the vessel wall.
- (4) The file prepared for FAVOR assumes that the code simulates flaws for the total vessel wall thickness, rather than just the category 1 and 2 regions which address only the inner 3/8 of the wall thickness. Terry will need to account for this concern during the FAVOR calculations

The resulting very large number of flaws (> 130,000) per vessel is based on a photograph of one small area of a vessel surface, with the implication that this area was representative of the entire vessel. It is possible that subclad flaws tend to occur in patches of the vessel surface. However it is generally understood that subclad flaws occur in a wide spread manner and that there are very large numbers of flaws given the conditions for subclad cracking exist. Based on PNNL's limited review of documents it

is difficult to justify reducing the estimated flaw density of subclad flaws. However, it would be useful to perform a sensitivity calculation to see if refinement of my estimate would have a significant effect on the FAVOR calculations.

BIBLIOGRAPHIC DATA SHEET

(See instructions on the reverse)

NUREG-1806, Vol.2

2. TITLE AND SUBTITLE

Technical Basis for Revision of the Pressurized Thermal Shock (PTS) Screening Limit in the PTS Rule (10 CFR 50.61): Appendices

3. DATE REPORT PUBLISHED

MONTH

YEAR

August

2007

4. FIN OR GRANT NUMBER

5. AUTHOR(S)

Mark EricksonKirk, Mike Junge, William Arcieri, B. Richard Bass, Robert Beaton, David Bessette, T.H.(James) Chang, Terry Dickson, C. Don Fletcher, Alan Kolaczowski, Shah Malik, Todd Mintz, Claud Pugh, Fredric Simonen, Nathan Siu, Donnie Whitehead, Paul Williams, Roy Woods, Sean Yin

6. TYPE OF REPORT

Technical

7. PERIOD COVERED (Inclusive Dates)

6-99 to 6-06

8. PERFORMING ORGANIZATION - NAME AND ADDRESS (If NRC, provide Division, Office or Region, U.S. Nuclear Regulatory Commission, and mailing address; if contractor, provide name and mailing address.)

Division of Fuel, Engineering, and Radiological Research
Office of Nuclear Regulatory Research
U.S. Nuclear Regulatory Commission
Washington, DC 20555-0001

9. SPONSORING ORGANIZATION - NAME AND ADDRESS (If NRC, type "Same as above"; if contractor, provide NRC Division, Office or Region, U.S. Nuclear Regulatory Commission, and mailing address.)

Division of Fuel, Engineering, and Radiological Research
Office of Nuclear Regulatory Research
U.S. Nuclear Regulatory Commission
Washington, DC 20555-0001

10. SUPPLEMENTARY NOTES

M. EricksonKirk, NRC Project Manager

11. ABSTRACT (200 words or less)

During plant operation, the walls of reactor pressure vessels (RPVs) are exposed to neutron radiation, resulting in localized embrittlement of the vessel steel and weld materials in the core area. If an embrittled RPV had a flaw of critical size and certain severe system transients were to occur, the flaw could very rapidly propagate through the vessel, resulting in a through-wall crack and challenging the integrity of the RPV. The severe transients of concern, known as pressurized thermal shock (PTS), are characterized by a rapid cooling of the internal RPV surface in combination with repressurization of the RPV. Advancements in our understanding and knowledge of materials behavior, our ability to realistically model plant systems and operational characteristics, and our ability to better evaluate PTS transients to estimate loads on vessel walls led the NRC to realize that the earlier analysis, conducted in the course of developing the PTS Rule in the 1980s, contained significant conservatisms.

This report summarizes 21 supporting documents that describe the procedures used and results obtained in the probabilistic risk assessment, thermal hydraulic, and probabilistic fracture mechanics studies conducted in support of this investigation. Recommendations on toughness-based screening criteria for PTS are provided.

12. KEY WORDS/DESCRIPTORS (List words or phrases that will assist researchers in locating the report.)

pressurized thermal shock, probabilistic fracture mechanics, nuclear reactor pressure vessel
pressurized water reactor

13. AVAILABILITY STATEMENT

unlimited

14. SECURITY CLASSIFICATION

(This Page)

unclassified

(This Report)

unclassified

15. NUMBER OF PAGES

16. PRICE